Modeling of Heat Transfer Coefficients during Condensation at Low Mass Fluxes Inside Horizontal and Inclined Smooth Tubes

Daniel Raphael Ejike Ewim, Mehdi Mehrabi, and Josua Petrus Meyer

Department of Mechanical and Aeronautical Engineering, University of Pretoria, Pretoria, South Africa

ABSTRACT

In this study, in-tube condensation was conducted for mass fluxes of 100, 75 and 50 kg/m^2s, and temperature differences of 1, 3, 5, 8 and 10 °C. Measurements and flow regimes were captured at various mean vapor qualities between 0.1 and 0.9 inside an inclined smooth tube with an inside diameter of 8.38 mm and 1.49 m long. Fifteen distinct inclination angles from -90° to 90° were considered while the condensation temperature was always maintained at 40 °C. The experimental results showed that the inclination angle significantly influenced the flow patterns and the heat transfer coefficients. It was also shown that the heat transfer coefficient was dependent on the temperature difference, even though this dependency was greater for downward flows than for upward flows. By using the experimental data and fuzzy C-means clustering adaptive neuro-fuzzy inference system (FCM-ANFIS) technique, a model was proposed for the prediction of heat transfer coefficients during condensation of low mass fluxes inside inclined smooth tubes. By using three statistical criteria, the performance of the proposed model was examined against experimental data and it was found that FCM-ANFIS was a strong tool for the prediction of the heat transfer coefficient based on the effective parameters of vapor quality, temperature difference and inclination angle.

Introduction

In-tube condensation finds application in refrigeration systems, heat pumps, power, nuclear and chemical industries. It has been thoroughly studied in the past (but not at low mass fluxes typically below 100 kg/m^2s in inclined smooth tubes). For this reason, it is important to thoroughly understand the two-phase flow process at low mass fluxes in the design and optimization of condensers. Studies may be experimental, theoretical, computational or analytical. The goal of these studies is to maximize heat transfer coefficients and minimize pressure drops.

Details of previous experimental studies can be found in [1–22]. According to these studies, at high mass fluxes, the heat transfer coefficients are mass flux dependent. On the other hand, studies at low mass fluxes reveal that temperature differences between the condensing wall and saturation temperatures of the condensing fluids play a pivotal role in the overall heat transfer process. The challenge with experimental work is that it is usually expensive to carry out because of the nature of the equipment and instrumentation needed. Furthermore, it may be time consuming and challenging. On the other hand, computational fluid dynamics work [23,24] is also in the development phase and no study has yet coupled the effect of temperature difference and inclination on heat transfer at low mass fluxes.

Soft computing and artificial intelligence (AI) methods have been touted as an optimization tool for the future. These methods are gaining magnificent grounds in a variety of engineering applications such as pattern recognition, decision-making, control systems, information processing, symbolic mathematics, computer vision and robotics. Artificial neural network (ANN) and adaptive neuro-fuzzy inference system (ANFIS) as soft computing tools have been used to successfully model, optimize and predict heat transfer coefficients and other thermal performance parameters in a variety of heat transfer applications [25–45]. The advantage of AI is that it is quicker and it allows the study of complex thermal systems that otherwise would have been impossible to characterize with conventional analytical or numerical techniques.

CONTACT Dr. Mehdi Mehrabi. Department of Mechanical and Aeronautical Engineering, University of Pretoria, Private Bag X20, Hatfield, Pretoria, 0028, South Africa. Email: mehdi.mehrabi@up.ac.za

Nomenclature

A	fuzzy set in ANFIS structure
A_{cs}	test section cross-sectional area [m^2]
A_i	internal surface area [m^2]
$a_{i,j}$	consequent parameter matrix
AI	artificial intelligence
$ANFIS$	adaptive neuro-fuzzy inference system
ANN	artificial neural network
B	fuzzy set in ANFIS structure
C	Gaussian membership function center
d_i	inlet diameter of test section tube [m]
f	outputs within the fuzzy region in ANFIS structure
FCM	fuzzy C-means clustering
G	mass flux [kg/m^{2}s]
h	heat transfer coefficient [W/m^{2}K]
L	length of test section [m]
M	multiplication function in ANFIS structure
$\dot{m}$	mass flow rate [kg/s]
MAE	mean absolute error
MF	fuzzy membership function
N	normalization function in ANFIS structure
MRE	mean relative error
n	number of data points
$\dot{Q}$	heat transfer rate [W]
$RMSE$	root mean square error
S	summation function in ANFIS structure
T	temperature [K]
T_{sat}	saturation temperature [K]
$\bar{T}_{w,i}$	average wall inner temperature [K]
w	firing strength in ANFIS structure
$\bar{w}$	normalized firing strength in ANFIS structure
x	input of ANFIS structure
X_a	actual (experimental) data
X_p	predicted value
y	input of ANFIS structure

Greek symbols

χ	vapor mass fraction
Θ	inclination angle [°]
σ	Gaussian membership function width

Subscripts

r,in	inlet refrigerant temperature
r,out	outlet refrigerant temperature
$w,test$	water side of the test section
$r,test$	refrigerant side of the test section

In general, AI studies with respect to heat exchangers are categorized into four major groups, namely (i) modeling of heat exchangers, (ii) estimation of heat exchanger parameters, (iii) estimation of phase change characteristics in heat exchangers and (iv) control of heat exchangers [42]. A review of these studies shows that ANN has been successfully used for a variety of heat transfer applications. However, no ANN study has coupled the combined effect of inclination and temperature difference for condensation inside inclined smooth tubes.

Azizi and Ahmaldoo [27] developed an ANN model to predict the convective heat transfer coefficients during the condensation of R134a inside inclined smooth tubes. They used the experimental data from the published work of Meyer et al. [14]. They concluded that the ANN model was able to predict the heat transfer coefficients over the entire range of inclination angles and independent of the flow pattern. However, their model did not consider the temperature difference effect, which was found [13,17,18,46] to influence the heat transfer at low mass fluxes.

Abadi et al. [47] used ANFIS for the optimization and prediction of pressure drops and heat transfer coefficients during the condensation of R134a in inclined smooth tubes. They examined the performance of three different ANFIS structure identification methods. For the training, they used the experimental data of [14,48,49]. They also compared their model with the numerical simulations. It was found that while the numerical simulations performed better than the proposed model, the errors of both ANFIS models were within the uncertainties of the experimental data. They also concluded that the ANFIS model was a useful tool in obtaining fast and reliable results.

Balcilar et al. [50] investigated the best ANN method to model the heat transfer coefficient and pressure drops during the condensation of R134a at high mass fluxes in a vertical smooth tube at two different saturation temperatures. They used the results of their experiments for the training and validation. They found that their model was able to predict the experimental condensation heat transfer coefficient and pressure drops with a deviation of ± 5% for all tested conditions.

Therefore, it can be concluded that no AI study has coupled the effect of temperature difference and inclination angles to describe the condensation heat transfer characteristics in the low mass flux region in smooth tubes covering the whole range of inclinations. This paper therefore studies the applicability of AI to model the effect of inclination and temperature difference, vapor quality and mass fluxes on heat transfer coefficients. It is a continuation (4th part) of the authors' previous works [13,17,18,51] where the heat transfer coefficients, pressure drops and flow patterns during condensation in smooth and inclined tubes were studied and reported.

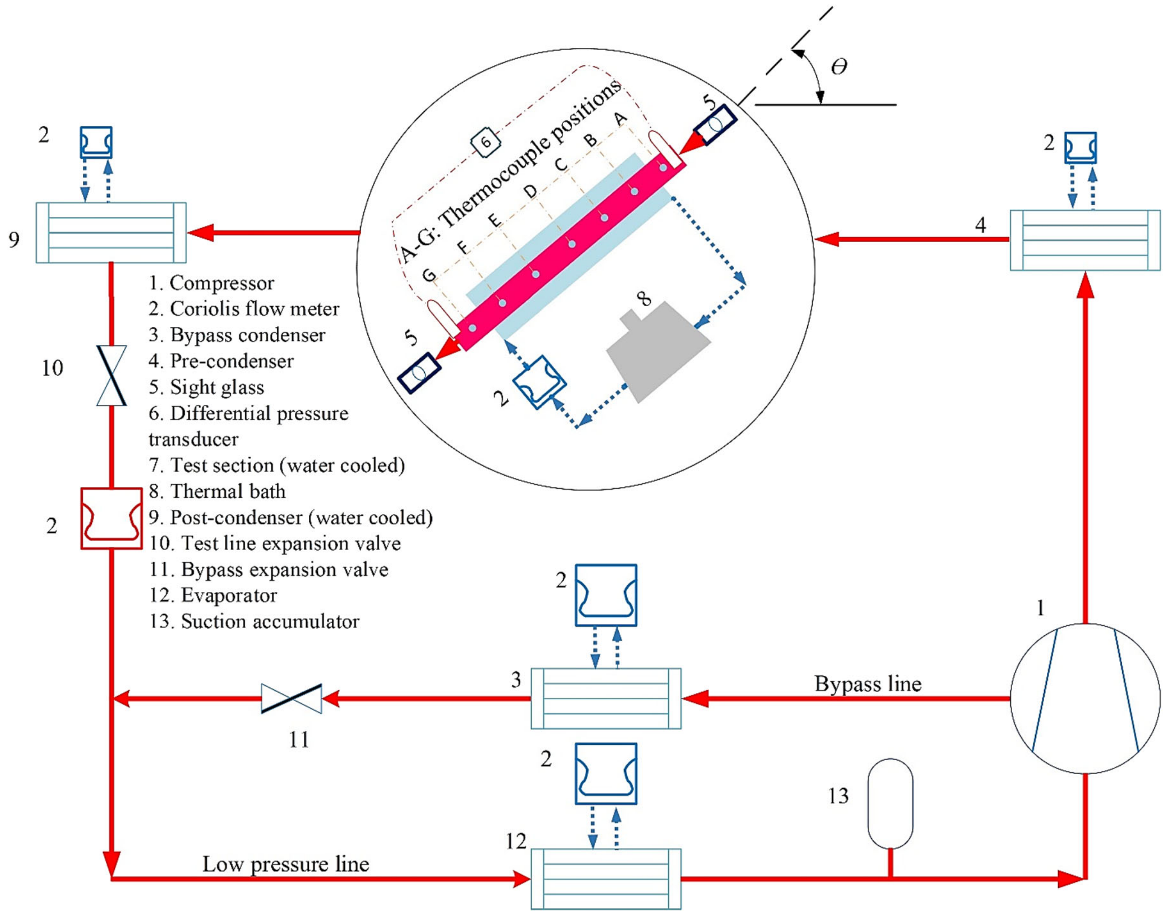

Figure 1. Schematic diagram of the experimental set-up and test section.

Experimental set-up

The set-up utilized for this study (Figure 1) is well known and was previously used for various condensation studies [13–15,18–20,46,48,49,51–56]. However, upgrades were made to cater for the low mass flux needs of this particular investigation as detailed in [13,17,18,46,51]. The experimental bench consisted of a refrigerant compression cycle (shown as solid lines in the figure) and various water cycles (shown as dashed lines in the figure). The angles of inclination (Θ) of the test condenser could be altered from −90° (downward flow) to 90° (upward flow), with 0° (horizontal flow) kept as the reference point. These angles were measured with an inclinometer, which was calibrated to an error of 0.01°. The internal tube of the test condenser was 1.49 m long with an inner diameter of 8.38 mm and an outer diameter of 9.54 mm. The annulus outer tube had an inner and outer diameter of 14.5 mm and 15.9 mm, respectively. The test, pre-, post- and bypass condensers, evaporator, and all refrigerant and water lines were insulated with 60 mm of a closed cell elastometric nitrile rubber, which had a thermal conductivity of 0.039 W/m.K. This was to prevent energy losses.

The data reduction of the heat transfer coefficients is exhaustively discussed in [13,18] and will not be repeated in this study. However, it should be noted that the “temperature differences” frequently used in the present study for the heat transfer coefficient calculations were:

$$\Delta T = T_{sat} - \overline{T}_{w,i} \tag{1}$$

They refer to the difference in temperature between the refrigerant condensation temperatures, T_{sat}, and mean wall inner temperatures, $\overline{T}_{w,i}$, of the test section. The condensation temperatures were the mean between the measured inlet, $T_{r,in}$, and outlet refrigerant temperature, $T_{r,out}$, measurements of the test condenser. The condensation temperature also corresponded to within 0.1 °C of the condensation temperature, which was obtained from REFPROP [57] when the absolute saturation pressure measurements taken from the mean of the entrance and exit test section pressure measurements were used.

The heat transfer coefficients were calculated as:

$$h = \frac{\dot{Q}_{w,test}}{A_i \Delta T} \tag{2}$$

The rate of heat transfer, $\dot{Q}_{w,test}$, of the water side of the test condenser was used to determine the heat transfer coefficients. The inner-surface area ($A_i = \pi d_i L$) of the test section of the heat transfer tube was determined from the measured tube inlet diameter, d_i, and the length of the test section over which the heat transfer occurred, L.

Finally, all the mass fluxes were calculated as:

$$G = \frac{\dot{m}_{r,test}}{A_{CS}} \tag{3}$$

where the area of test section cross-section was calculated as $A_{cs} = (\pi/4)d_i^2$.

Neural and neuro-fuzzy networks

An artificial neural network is a calculation tool, which is used to test the data and to create a model by these data. When a neural network applies the training data for learning latent patterns existing within the data, it may use them to access the outputs. Regarding the researchers' objectives, various kinds of artificial neural networks may be used. One of the most well-known artificial neural networks is the multilayer feed-forward neural network, which is a neural network with a supervised learning. This neural network is useful for solving the problems that include learning the relationship between definite input and output sets. In the error backpropagation algorithm, the network creates an output (or an output set) for the provided input criterion and compares the reaction with the appropriate reaction of each neuron. Then the weights of the network are corrected to reduce the error and the next criterion is emerged. The weights will be corrected continuously, until the total errors are less than the authorized error value. Because this algorithm has a descending gradient in the error function, the inputs correction gradually minimizes the mean square error [58–60].

In moving forward, the neuro-fuzzy networks normally calculate the node outputs up to the last layer in every period of instruction. Thus, the resultant parameters are calculated by the least squares error method. After calculating the error in the returning backward route, the error ratios are distributed on condition parameters and their values are corrected by the error descending gradient method. Various structures have been suggested to establish a fuzzy system by neural networks. One of the most powerful structures developed by Jang [61] is known as ANFIS. The main instruction approach in this structure is error backpropagation, which scatters the error value toward inputs by algorithm of the steepest gradient descent and corrects the parameters.

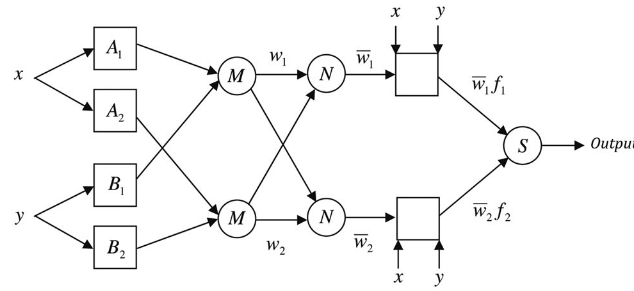

Figure 2. Schematic of the ANFIS architecture.

Architecture of ANFIS

An ANFIS system is built based on a combination of ANN and fuzzy logic techniques. This combination creates robust modeling for many different engineering problems. In an ANFIS network, an ANN is used to find the appropriate membership functions and reduce the rate of errors in the rule determination process [62]. On the other hand, a rule-based fuzzy inference system in an ANFIS system transfers qualitative knowledge into an accurate quantitative analysis. The ANFIS structure consists of five distinct layers shown in Figure 2.

The first layer of the ANFIS structure combines all input and output data into a single input-output space, and applies the fuzzification later. The firing strength of a rule is calculated in the second layer, which is called the "rule layer". This layer connects each node of the second layer with a fuzzy rule. The third layer conducts a normalization of the membership functions by calculating the rate of the firing strength associated with each rule for a summation of all rule firing strengths. Defuzzification occurs in the fourth layer, which is the conclusive part of the fuzzy rules. Consequent parameters of the fuzzy rules are calculated in this layer. Finally, the last layer calculates the network outputs. Detailed information regarding the ANFIS is provided in the previous works of the authors [63–68].

Fuzzy C-means (FCM) clustering structure identification method

Grid partitioning, subtractive clustering method and fuzzy C-means clustering (FCM) are three structure identification methods commonly used in an ANFIS system. The selection of input variables, input space partitioning, the membership functions and creation of the fuzzy rules as well as selection of the initial parameters for membership functions all take place during the structure identification process [47,69,70].

In this paper, the fuzzy C-means clustering method was used as the ANFIS structure identification. This algorithm was initially introduced by Dunn [71], Bezdek [72] and Bezdek et al. [73] as a data clustering technique in which each data point belongs to two or more clusters. The purpose of this algorithm was to determine cluster centers based on the minimization of the sum of the weighted squares distance between each data point and the cluster centers. In this algorithm, the number of clusters and the fuzziness index are first selected randomly. The algorithm then begins by initializing the cluster centers using a random value from the data points. In the next step, the membership matrix and the objective function are computed. Finally, the new fuzzy cluster centers are computed. This iterative process is continued until the objective function is lower than the termination criteria. Detailed information about the FCM identification method is provided by the present authors in References [63,64,66–68].

Result and discussion

Results of experimental studies

The results of the experiments are detailed in Ewim et al. [13]. The general trend found in the experimental study is shown in Figures 3–5. The figures show the inclination effect on the measured heat transfer coefficients at different temperatures at a mean vapor quality of 0.5 and mass fluxes of 100, 75 and 50 kg/m^{2}s. The three figures indicate that the highest heat transfer coefficient was obtained at the lowest temperature difference tested per data point and at inclination angles of either $-15°$ or $-30°$ (downward flow). On the other hand, the lowest heat transfer coefficients were consistently found at the highest temperature difference tested per data point and at an inclination angle of $-90°$ (vertical downward flow). It was also found that even though the heat transfer coefficients for an inclination angle of $-90°$ increased with a decrease in temperature difference, this difference was about 2% (negligible). The opposite was found for vertical upward flows. It was also found

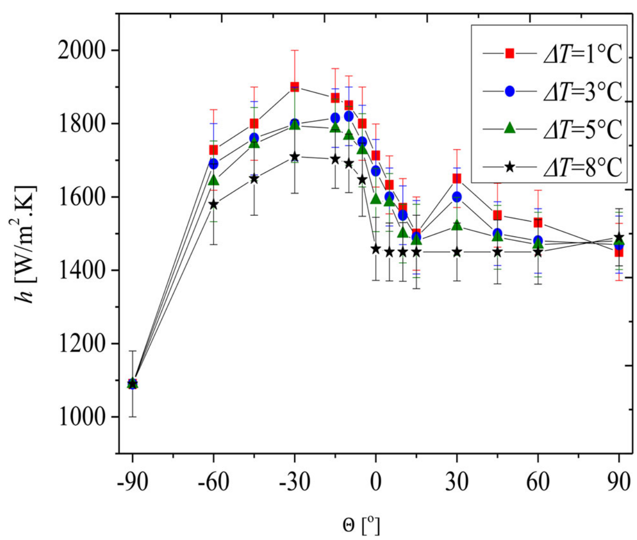

Figure 4. Experimental condensation heat transfer coefficients as a function of inclination angle at G = 75 kg/m^{2}s, $\chi = 0.5$, and different wall and refrigerant temperatures.

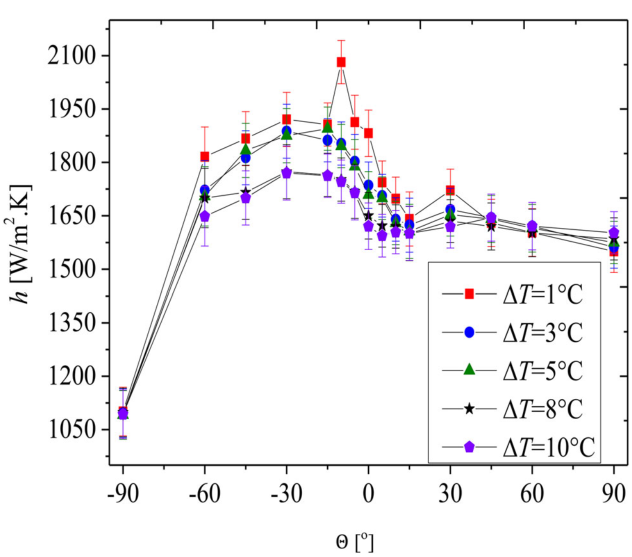

Figure 3. Experimental condensation heat transfer coefficients as a function of inclination angle at G = 100 kg/m^{2}s, $\chi = 0.5$, and different wall and refrigerant temperatures.

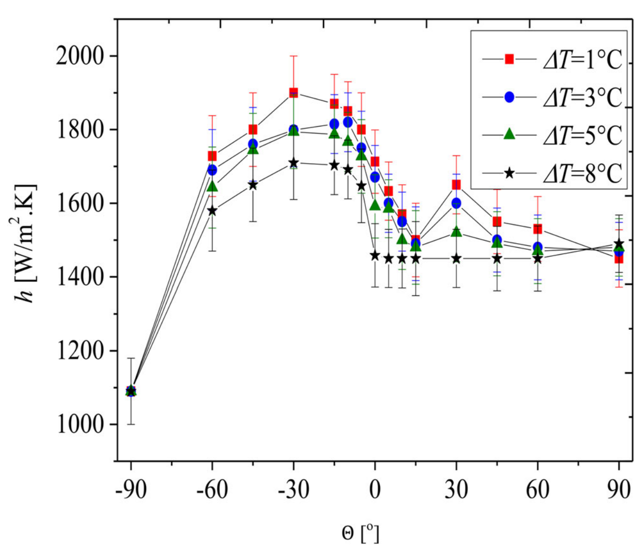

Figure 5. Experimental condensation heat transfer coefficients as a function of inclination angle at G = 50 kg/m^{2}s, $\chi = 0.5$, and different wall and refrigerant temperatures.

that the inclination effect on the heat transfer coefficients were more noticeable for downward flows than for upward flows. The trend in the variations in heat transfer coefficients could be linked to the prevailing flow pattern. For instance, during vertical downward flows, the flow pattern was churn, which generally corresponded to low heat transfer coefficients. With an increase in the inclination angle to between $-15°$ and $-30°$, the flow regime became stratified wavy and as a result, there was an increase in the heat transfer coefficients. With an additional increase in the inclination angle, there was an increase in the liquid film thickness, which led to an increase in the heat transfer resistance and consequently a reduction in the heat transfer coefficient.

When stratified smooth flow and stratified wavy flow occurred, the inclination angles had a heat transfer enhancement effect. As the inclination angles decreased from $0°$ to $-30°$, the liquid film thickness decreased because of the gravity and consequently led to an increase in the convection effect. As a result, the thermal resistance decreased, and therefore, the heat transfer coefficient increased. Furthermore, the flow regimes were almost the same for this region (stratified wavy or stratified.) With a further decrease of the inclination angle from $-30°$ to $-60°$, the flow regime remained stratified wavy and the liquid film thickness did not change significantly; therefore, the heat transfer coefficient remained almost unchanged between these two inclination angles. However, with the decrease in the inclination angle from $-60°$ to $-90°$, there was a change in the flow regime from stratified wavy to either churn, intermittent or annular flows. When the flow regime changed to churn or intermittent flows, the liquid phase covered the tube surface sporadically, which caused an increase in thermal resistance and consequently a decrease in the heat transfer coefficients. However, when the flow regime changed to annular flow, the liquid film always covered the entire tube surface, which also caused a significant decrease in the heat transfer coefficients. The same interpretation is valid for the upward flow directions, but the difference is that in those regions, the flow regimes were always intermittent or churn, for which the inclination had no significant effect on the heat transfer coefficients. For the vertical upward flows, the flow regimes were almost churn and therefore the heat transfer coefficients decreased, while the inclination effect was non-existent. For upward flows, there was no noticeable effect of inclination on the heat transfer coefficients at the different temperatures. Furthermore, it was noticed that the effect of temperature difference was different for the vertical upward ($+90°$) flow in comparison with the vertical downward ($-90°$) flow.

When comparing the heat transfer coefficients of the horizontal tube ($0°$) orientation with those of the downward vertical ($-90°$) orientation, it was found that the heat transfer coefficients of the horizontal orientation were greater. This could be ascribed to the stratification due to gravity, which enhanced the heat transfer by keeping the condensate thickness low in the upper region of the tube in comparison with the case of vertical downward flow. In this case, even though the heat transfer coefficient at the bottom was lower, the heat transfer enhancement in the upper region prevailed and the average cross-sectional heat transfer coefficient was increased in comparison with the case of the vertical downward flow orientation. To conclude, it was confirmed that the condensation heat transfer coefficients were more responsive to variations in the inclination angles near the horizontal orientation. In these slightly tilted positions (either upward or downward), the flow patterns were found to be either stratified wavy or stratified smooth.

Validation of the proposed ANFIS models

A total number of 525 input-output experimental data points obtained from the authors' previous works [13,17,18,46] were used to predict the condensation heat transfer coefficient of low mass fluxes in an inclined smooth tube. The experimental data were divided into two subsets as 405 data points for training and 120 data points for testing purposes. The optimum ANFIS structure and the membership functions were obtained by the FCM structure identification method in which the input variables were fuzzified with Gaussian membership functions labeled MF1-MF28. The parameters of these membership functions are given in Table 1. The optimum consequent parameters ($a_{i,j}$) obtained after the ANFIS training are given in Appendix. Three statistical criteria, namely the mean absolute error (*MAE*), mean relative error (*MRE*) and root mean square errors (*RMSE*), were used as given in Table 2 to show the accuracy of the proposed FCM-ANFIS models to predict the condensation heat transfer coefficient of low mass fluxes in an inclined smooth tube.

Figure 6 compares the predicted results of the FCM-ANFIS model with the experimental results of the condensation heat transfer coefficient for two cases of $G = 75\,\mathrm{kg/m^2s}$, $\chi = 0.5$, $\Delta T = 5\,°\mathrm{C}$ and $G = 75\,\mathrm{kg/m^2s}$, $\chi = 0.75$, $\Delta T = 3\,°\mathrm{C}$. The plot shows

Table 1. Parameters of ANFIS membership functions for the modeling of the condensation heat transfer coefficient in low mass fluxes.

	Input 1 G (kg/m^2.s)		Input 2 x		Input 3 ΔT		Input 4 θ	
Membership function	σ	C	σ	C	σ	C	σ	C
MF1	8.607	56.14	0.04456	0.5227	0.7233	3.347	12.52	19.93
MF2	7.864	65.32	0.1395	0.6528	0.9567	3.709	12.47	−15.34
MF3	6.769	96.01	0.05391	0.5712	0.961	6.276	11.61	−6.943
MF4	8.476	57.4	0.02091	0.5507	0.7911	2.594	11.76	14.09
MF5	6.566	94.03	0.01888	0.3432	0.6735	4.523	11.5	12.66
MF6	8.215	60.68	0.05007	0.5063	0.975	3.939	11.36	−2.423
MF7	5.999	71.99	0.07658	0.595	0.8145	3.774	18.83	56.78
MF8	6.636	86.61	0.07655	0.4815	1.038	6.678	12.6	−15.82
MF9	5.583	73.05	0.1066	0.3	0.8544	3.933	25.7	85.98
MF10	8.358	52.14	0.07782	0.3474	0.8222	3.417	16.87	52.21
MF11	5.669	92.34	0.02749	0.677	0.9053	1.926	10.62	−13.5
MF12	7.694	64	0.0553	0.3999	0.7043	4.459	17.36	−44.72
MF13	6.718	97.72	0.04038	0.4001	1.133	7.114	11.69	10.69
MF14	6.407	94.74	0.0567	0.4944	0.9262	4.012	11.98	−16.8
MF15	5.843	74.84	0.1041	0.5352	0.9743	4.491	12.75	−19.01
MF16	6.668	93.2	0.03034	0.3844	1.171	6.261	19.28	−53.07
MF17	5.852	66.43	0.06478	0.3968	0.8537	4.491	23.6	−89.97
MF18	6.353	89.3	0.06611	0.6202	1.187	6.597	17.81	45.15
MF19	5.591	99.76	0.03213	0.6098	1.017	6.713	24.1	−89.96
MF20	4.737	77.45	0.04323	0.5739	0.7245	4.181	24.09	−89.93
MF21	5.946	98.46	0.06805	0.7493	0.9486	2.237	10.73	6.78
MF22	6.127	70.38	0.02848	0.3418	0.8457	5.549	11.15	11.38
MF23	6.25	98.27	0.05082	0.6447	0.8436	2.763	14.12	28.34
MF24	7.878	51.49	0.01763	0.5625	0.6949	3.022	23.98	−89.94
MF25	6.053	74.19	0.05002	0.3845	0.7447	5.04	11.64	−3.972
MF26	6.562	99.05	0.04954	0.4913	0.9627	6.204	19.44	56.49
MF27	5.787	79.6	0.09433	0.255	0.9665	5.176	13.76	31.86
MF28	6.253	71.46	0.1402	0.7056	1.036	4.197	11.26	5.363
MF29	5.476	99.93	0.00865	0.7015	0.9232	1.483	11.56	−23.82

σ represents Gaussian MFs width and C determines Gaussian MFs center.

Table 2. Statistical criteria used for the analysis of the results.

Statistical criterion	Equation
Mean absolute error	$MAE = \frac{1}{n}\sum_{i=1}^{n} \lvert X_p - X_a \rvert$
Mean relative error	$MRE(\%) = \frac{100}{n}\sum_{i=1}^{n}\left(\frac{\lvert X_p - X_a \rvert}{X_a}\right)$
Root mean square error	$RMSE = \sqrt{\frac{1}{n}\sum_{i=1}^{n}(X_p - X_a)^2}$

X_p is the predicted value, X_a is the actual (experiment) data, and n is the number of data points.

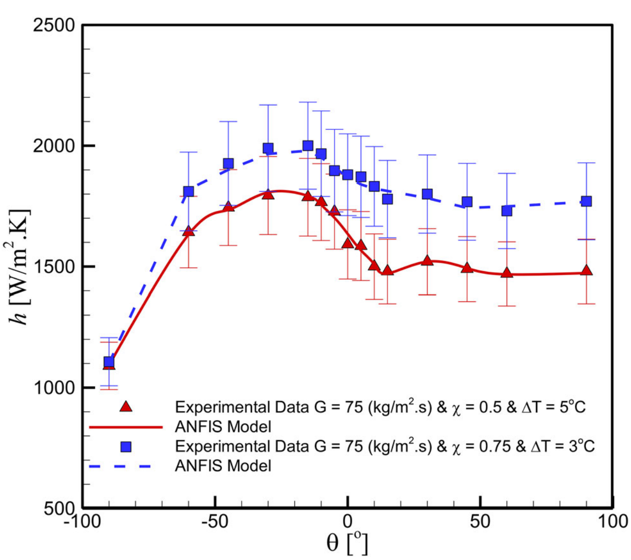

Figure 6. Comparison between the performances of the proposed ANFIS models for the prediction of condensation heat transfer coefficient for G = 75 kg/m^{2}s and $\chi = 0.5$ and 0.75, and $\Delta T = 3$ and 5 °C.

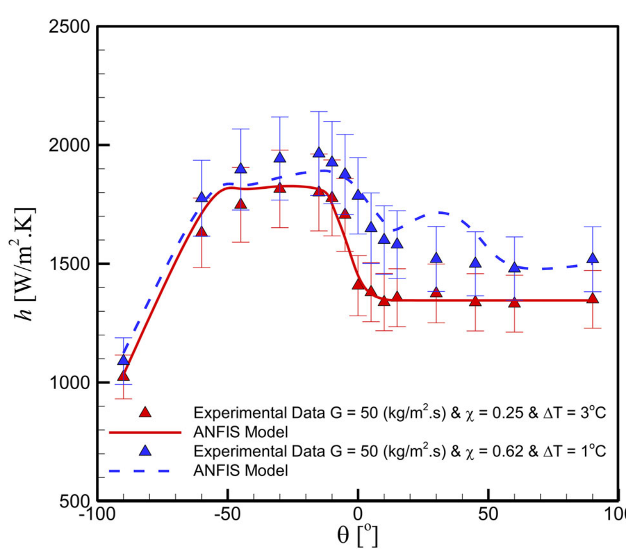

Figure 7. Comparison between the performances of the proposed ANFIS models for the prediction of condensation heat transfer coefficient for G = 50 kg/m^{2}s and $\chi = 0.25$ and 0.62, and $\Delta T = 1$ and 3 °C.

that the proposed model for both cases is in excellent agreement with the experimental data ($MAE = 11.27$, $MRE = 0.7\%$ and $RMSE = 15.52$) and ($MAE = 17.58$, $MRE = 0.96\%$ and $RMSE = 19.74$).

Figure 7 shows the results of the condensation heat transfer coefficient using the proposed model

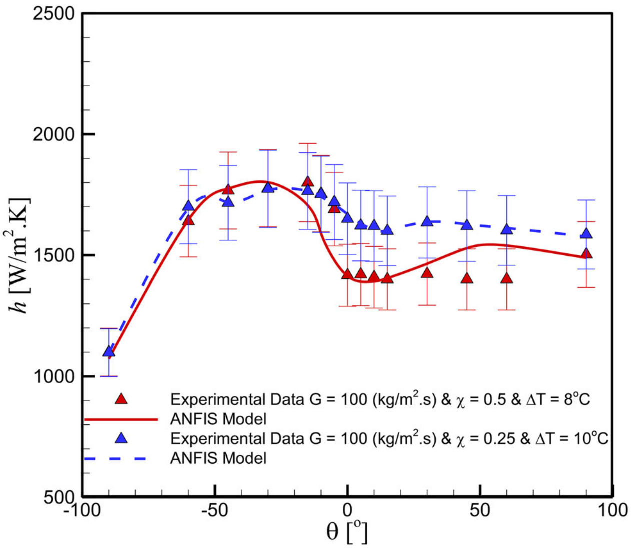

Figure 8. Comparison between the performances of the proposed ANFIS models for the prediction of condensation heat transfer coefficient for $G = 100\,\text{kg/m}^2\text{s}$ and $\chi = 0.25$ and 0.5, and $\Delta T = 8$ and $10\,°\text{C}$.

for two cases of $G = 50\,\text{kg/m}^2\text{s}$, $\chi = 0.25$, $\Delta T = 3\,°\text{C}$ and $G = 50\,\text{kg/m}^2\text{s}$, $\chi = 0.62$, $\Delta T = 1\,°\text{C}$ compared with the experimental results. The accuracy of the proposed model to predict the experimental data is good in two cases ($MAE = 29.03$, $MRE = 1.85\%$ and $RMSE = 41$) and ($MAE = 62.83$ $MRE = 3.85\%$ and $RMSE = 78.83$). The performance of the proposed FCM-ANFIS is not as great as the result of Figure 6, but still is in a very reliable range. The model cannot predict the condensation heat transfer coefficient of $G = 50\,\text{kg/m}^2\text{s}$, $\chi = 0.62$, $\Delta T = 1\,°\text{C}$ for the inclination angles between $\theta = 10°$ and $\theta = 45°$. The reason for this behavior could be related to the lack of training data for the mentioned range of inclination angles.

In Figure 8, the experimental results for the condensation heat transfer coefficient are compared with those of the proposed FCM-ANFIS model for two cases of $G = 100\,\text{kg/m}^2\text{s}$, $\chi = 0.25$, $\Delta T = 10\,°\text{C}$ and $G = 100\,\text{kg/m}^2\text{s}$, $\chi = 0.5$, $\Delta T = 8\,°\text{C}$ respectively. While the model performs the best for the case of $G = 100\,\text{kg/m}^2\text{s}$, $\chi = 0.25$, $\Delta T = 10\,°\text{C}$ ($MAE = 7.18$, $MRE = 0.44\%$ and $RMSE = 8.88$), it fails to predict the condensation heat transfer coefficient for the case of $G = 100\,\text{kg/m}^2\text{s}$, $\chi = 0.5$, $\Delta T = 8\,°\text{C}$ and for inclination angles between $\theta = 10°$ and $\theta = 60°$ with high accuracy. However, the overall accuracy of the proposed model is still very good for the case of $G = 100\,\text{kg/m}^2\text{s}$, $\chi = 0.5$, $\Delta T = 8\,°\text{C}$ ($MAE = 60.91$, $MRE = 3.91\%$ and $RMSE = 89.67$) since the relative error is lower than 4 percent.

Conclusions

Experiments were conducted during the in-tube condensation of R134a in an inclined smooth tube at mass fluxes of 50, 75 and $100\,\text{kg/m}^2\text{s}$. The average vapor qualities considered were between 10% and 90% at temperature differences of 1, 3, 5, 8 and $10\,°\text{C}$. Based on the experimental results, a model based on FCM-ANFIS was proposed for the prediction of the condensation heat transfer coefficient at low mass fluxes of R134a in an inclined tube.

Based on this study, the following conclusions are made:

I. The optimum condensation heat transfer coefficients were found at the lowest temperature differences tested per data point and at inclination angles between $-15°$ and $-30°$.

II. The condensation heat transfer coefficient was a function of the circumference occupied by the condensation film and its thickness, primarily a function of the angle of inclination and temperature difference.

III. The comparison between the experimental data and the result of the proposed FCM-ANFIS model showed that the proposed model could predict the heat transfer coefficient condensation inside an inclined smooth tube very well.

IV. The result of the proposed model also showed that the FCM-ANFIS technique was a very useful method that could help us to find the condensation heat transfer coefficient of low mass fluxes of R134a in an inclined smooth tube fast with a high level of accuracy. In all tested cases, the deviation of the predicted result was not more than 5 percent of the experimental data.

Notes on contributors

Daniel R. E. Ewim obtained his B.Eng. in Mechanical Engineering (Refrigeration & Air-Conditioning Engineering) in 2006 from the Federal University of Technology Owerri, Nigeria and his M.Eng. in Mechanical Engineering (Energy Studies) in 2012, from the University of Agriculture, Makurdi, Nigeria. He is currently completing his Ph.D. in Mechanical Engineering at the University of Pretoria, South Africa. He is a member of the Clean Energy Research Group at the University of Pretoria and his research interests include thermofluids, nanofluids, nuclear thermohydraulics, clean energy, CFD, refrigeration and engineering education.

Mehdi Mehrabi obtained his B.Eng. in Mechanical Engineering (Heat and Fluid Flow) in 2006 and his M.Eng. in Mechanical Engineering (Energy Conversion) in 2011, both from Urmia University, Urmia, Iran, and his Ph.D. in Mechanical Engineering from the University of Pretoria, South Africa in 2015. He joined the Department of Mechanical and Aeronautical Engineering at the University of Pretoria, South Africa as a Senior Lecturer in 2017. He is a member of the Clean Energy Research Group and his research interests include convection heat transfer, multi-objective optimization techniques, application of artificial intelligence techniques for modeling heat transfer processes, clean and renewable energy and thermophysical properties of nanofluids.

Josua P. Meyer is Professor and Head of the Department of Mechanical and Aeronautical Engineering and Chair of the School of Engineering at the University of Pretoria. His research field is convective heat transfer in which he has published more than 600 scholarly articles, conference papers and book chapters. He has received various international awards for his research. According to the Essential Science Indicators of the ISI Web of Knowledge he is ranked among the top 1% of the world in engineering in all three evaluation fields, which are citations, number of papers and citations per paper. He is/was the editor, lead editor and associate editor of various prominent international heat transfer journals.

References

[1] J. S. Shin, and M. H. Kim, "An experimental study of flow condensation heat transfer inside circular and rectangular mini-channels," *Heat Transf. Eng.*, vol. 26, no. 3, pp. 36–44, Sep. 2005. DOI: 10.1080/01457630590907185.

[2] M. Christians, M. Habert, and J. R. Thome, "Film condensation of R-134a and R-236fa, part 2: Experimental results and predictive correlation for bundle condensation on enhanced tubes," *Heat Transf. Eng.*, vol. 31, no. 10, pp. 809–820, Jul. 2010.

[3] J. Palen, G. Breber, and J. Taborek, "Prediction of flow regimes in horizontal tube-side condensation," *Heat Transf. Eng.*, vol. 1, no. 2, pp. 47–57, Apr. 1979.

[4] T. Ji, L. Liebenberg, and J. P. Meyer, "Heat transfer enhancement during condensation in smooth tubes with helical wire inserts," *Heat Transf. Eng.*, vol. 30, no. 5, pp. 337–352, Jul. 2009. DOI: 10.1080/01457630802414466.

[5] J.-P. Bukasa, L. Liebenberg, and J. P. Meyer, "Influence of spiral angle on heat transfer during condensation inside spiralled micro-fin tubes," *Heat Transf. Eng.*, vol. 26, no. 7, pp. 11–21, 2005. Aug DOI: 10.1080/01457630590959278.

[6] J.-P. M. Bukasa, L. Liebenberg, and J. P. Meyer, "Heat transfer performance during condensation inside spiralled micro-fin tubes," *J. Heat Transf.*, vol. 126, no. 3, pp. 321–321, Jul. 2004. DO1:

[7] S. Garimella, "Condensation flow mechanisms in microchannels: Basis for pressure drop and heat transfer models," *Heat Transf. Eng.*, vol. 25, no. 3, pp. 104–116, Jul. 2004.

[8] G. A. Longo, S. Mancin, G. Righetti, and C. Zilio, "Saturated vapour condensation of R410A inside a 4 mm ID horizontal smooth tube: Comparison with the low GWP substitute R32," *Int. J. Heat Mass Transf.*, vol. 125, pp. 702–709, Oct. 2018.

[9] A. Cavallini *et al.*, "Condensation in horizontal smooth tubes: A new heat transfer model for heat exchanger design," *Heat Transf. Eng.*, vol. 27, no. 8, pp. 31–38, Sep. 2006,

[10] A. S. Dalkilic, and S. Wongwises, "Experimental study on the modeling of condensation heat transfer coefficients in high mass flux region of refrigerant HFC-134a inside the vertical smooth tube in annular flow regime," *Heat Transf. Eng.*, vol. 32, no. 1, pp. 33–44, Nov. 2011. DOI: 10.1080/01457631003732839.

[11] L. P.-W, M. Chen, and W.-Q. Tao, "Theoretical analysis and experimental investigation on local heat transfer characteristics of HFC-134a forced-convection condensation inside smooth horizontal tubes," *Heat Transfer Eng.*, vol. 21, no. 6, pp. 34–43, Oct. 2010. DOI: 10.1080/01457630050194799.

[12] M. Valinčius, M. Šeporaitis, E. Ušpuras, and A. Kaliatka, "Experimental investigation and RELAP5 modeling of two-phase flow in horizontal rectangular channel," *Heat Transf. Eng.*, vol. 32, no. 11-12, pp. 1026–1030, Jun. 2011. DOI: 10.1080/01457632.2011.556490.

[13] D. R. E. Ewim, J. P. Meyer, and S. M. A. Noori Rahim Abadi, "Condensation heat transfer coefficients in an inclined smooth tube at low mass fluxes," *Int. J. Heat Mass Transf.*, vol. 123, pp. 455–467, 2018. Aug. DOI: 10.1016/j.ijheatmasstransfer.2018.02.091.

[14] J. P. Meyer, J. Dirker, and A. O. Adelaja, "Condensation heat transfer in smooth inclined tubes for R134a at different saturation temperatures," *Int. J. Heat Mass Transf.*, vol. 70, pp. 515–525, Mar. 2014. DOI: 10.1016/j.ijheatmasstransfer.2013.11.038.

[15] S. Lips, and J. P. Meyer, "Experimental study of convective condensation in an inclined smooth tube. Part I: Inclination effect on flow pattern and heat transfer coefficient," *Int. J. Heat Mass Transf.*, vol. 55, no. 1–3, pp. 395–404, Jan. 2012.

[16] A. Cavallini, S. Bortolin, D. Del Col, M. Matkovic, and L. Rossetto, "Condensation heat transfer and pressure losses of high- and low-pressure refrigerants flowing in a single circular minichannel," *Heat Transf. Eng*, vol. 32, no. 2, pp. 90–98, Oct. 2011.

[17] D. R. E. Ewim, R. Kombo, and J. P. Meyer, "Flow pattern and experimental investigation of heat transfer coefficients during the condensation of R134a at low mass fluxes in a smooth horizontal tube," presented at the 12th International Conference on Heat Transfer, Fluid Mechanics and Thermodynamics

(HEFAT), Costa del Sol, Malaga, Spain, Jul. 11-13, 2016.

[18] J. P. Meyer, and D. R. E. Ewim, “Heat transfer coefficients during the condensation of low mass fluxes in smooth horizontal tubes,” *Int. J. Multiph. Flow*, vol. 99, pp. 485–499, Feb. 2018. DOI: 10.1016/j.ijmultiphaseflow.2017.11.015.

[19] R. Suliman, L. Liebenberg, and J. P. Meyer, “Improved flow pattern map for accurate prediction of the heat transfer coefficients during condensation of R-134a in smooth horizontal tubes and within the low-mass flux range,” *Int. J. Heat Mass Transf.*, vol. 52, no. 25–26, pp. 5701–5711, Dec. 2009. DOI: 10.1016/j.ijheatmasstransfer.2009.08.017.

[20] R. Suliman, M. Kyembe, and J. P. Meyer, “Experimental investigation and validation of heat transfer coefficients during condensation of R-134a at low mass fluxes,” presented at the 7th International Conference on Heat Transfer, Fluid Mechanics and Thermodynamics (HEFAT), Antalya, Turkey, Jul. 19–21, 2010.

[21] H.-S. Lee, and C.-H. Son, “Condensation heat transfer and pressure drop characteristics of R-290, R-600a, R-134a and R-22 in horizontal tubes,” *Heat Mass Transf.*, vol. 46, no. 5, pp. 571–584, 2010. DOI: 10.1007/s00231-010-0603-9.

[22] C. Aprea, A. Greco, and G. P. Vanoli, “Condensation heat transfer coefficients for R22 and R407C in gravity driven flow regime within a smooth horizontal tube,” *Int. J. Refrig.*, vol. 26, no. 4, pp. 393–401, Jun. 2003. DOI: 10.1016/S0140-7007(02)00151-2.

[23] S. M. A. Noori Rahim Abadi, J. P. Meyer, and J. Dirker, “Effect of inclination angle on the condensation of R134a inside an inclined smooth tube,” *Chem. Eng. Res. Des.*, vol. 132, pp. 346–357, Apr. 2018. DOI: 10.1016/j.cherd.2018.01.044.

[24] S. M. A. Noori Rahim Abadi, M. Mehrabi, and J. P. Meyer, “Numerical study of steam condensation inside a long, inclined, smooth tube at different saturation temperatures,” *Int. J. Heat Mass Transf.*, vol. 126, pp. 15–25, Nov. 2018.

[25] R. Romero-Méndez, P. Lara-Vázquez, F. Oviedo-Tolentino, H. M. Durán-García, F. G. Pérez-Gutiérrez, and A. Pacheco-Vega, “Use of artificial neural networks for prediction of the convective heat transfer coefficient in evaporative mini-tubes,” *Ing. Investig. Tecnol.*, vol. 17, no. 1, pp. 23–34, Jan.–Mar. 2016.

[26] S. Azizi, E. Ahmadloo, and M. M. Awad, “Prediction of void fraction for gas-liquid flow in horizontal, upward and downward inclined pipes using artificial neural network,” *Int. J. Multiph. Flow*, vol. 87, pp. 35–44, Dec. 2016.

[27] S. Azizi, and E. Ahmadloo, “Prediction of heat transfer coefficient during condensation of R134a in inclined tubes using artificial neural network,” *Appl. Therm. Eng.*, vol. 106, pp. 203–210, Aug. 2016. DOI: 10.1016/j.applthermaleng.2016.05.189.

[28] M. Boostani, H. Karimi, and S. Azizi, “Heat transfer to oil-water flow in horizontal and inclined pipes: Experimental investigation and ANN modeling,” *Int. J. Therm. Sci*, vol. 111, pp. 340–350, Jan. 2017. DOI: 10.1016/j.ijthermalsci.2016.09.005.

[29] G. Scalabrin, M. Condosta, and P. Mari, “Mixtures flow boiling: Modeling heat transfer through artificial neural networks,” *Int. J. Therm. Sci.*, vol. 45, no. 7, pp. 664–680, Jul. 2006. DOI: 10.1016/j.ijthermalsci.2005.09.011.

[30] M. A. Hamdan, E. A. Abdelhafez, A. M. Hamdan, and R. A. Haj Khalil, “Heat transfer analysis of a flat-plate solar air collector by using an artificial neural network,” *J. Infr. Syst.*, vol. 22, no. 4, pp. A4014004-1–A4014004-7, Dec. 2016. DOI: 10.1061/(asce)is.1943-555x.0000213.

[31] M. Balcilar, A. S. Dalkilic, O. Agra, S. O. Atayilmaz, and S. Wongwises, “A correlation development for predicting the pressure drop of various refrigerants during condensation and evaporation in horizontal smooth and micro-fin tubes,” *Int. Commun. Heat Mass Transf.*, vol. 39, no. 7, pp. 937–944, Aug.2012.

[32] Q. Wang, G. Xie, M. Zeng, and L. Luo, “Prediction of heat transfer rates for shell-and-tube heat exchangers by artificial neural networks approach,” *J. Therm. Sci.*, vol. 15, no. 3, pp. 257–262, Sep. 2006. DOI: 10.1007/s11630-006-0257-6.

[33] H. Salehi, S. Zeinali Heris, M. K. Salooki, and S. H. Noei, “Designing a neural network for closed thermosyphon with nanofluid using a genetic algorithm,” *Braz. J. Chem. Eng.*, vol. 28, no. 1, pp. 157–168, Jan./Mar. 2011.

[34] L. V. Kamble, D. R. Pangavhane, and T. P. Singh, “Artificial neural network based prediction of heat transfer from horizontal tube bundles immersed in gas-solid fluidized bed of large particles,” *J. Heat Transf.*, vol. 137, no. 1, pp. 012901–012901-9, Jan. 2015. DOI: 10.1115/1.4028645.

[35] T. N. Verma, P. Nashine, D. V. Singh, T. S. Singh, and D. Panwar, “ANN: Prediction of an experimental heat transfer analysis of concentric tube heat exchanger with corrugated inner tubes,” *Appl. Therm. Eng.*, vol. 120, pp. 219–227, Jun. 2017.

[36] G. Díaz, M. Sen, K. T. Yang, and R. L. McClain, “Simulation of heat exchanger performance by artificial neural networks,” *HVAC&R Res.*, vol. 5, no. 3, pp. 195–208, Feb. 2011. DOI: 10.1080/10789669.1999.10391233.

[37] W. Yaïci, and E. Entchev, “Performance prediction of a solar thermal energy system using artificial neural networks,” *Appl. Therm. Eng*, vol. 73, no. 1, pp. 1348–1359, Dec. 2014. DOI: 10.1016/j.applthermaleng.2014.07.040.

[38] C. Shen, L. Yang, X. Wang, Y. Jiang, and Y. Yao, “Predictive performance of a wastewater source heat pump using artificial neural networks,” *Build. Serv. Eng. Res. Tech.*, vol. 36, no. 3, pp. 331–342, Aug. 2015. DOI: 10.1177/0143624414547966.

[39] M. R. Jafari Nasr, A. H. Khalaj, and S. H. Mozaffari, “Modeling of heat transfer enhancement by wire coil inserts using artificial neural network analysis,” *Appl. Therm. Eng.*, vol. 30, no. 2-3, pp. 143–151, Feb. 2010. DOI: 10.1016/j.applthermaleng.2009.07.014.

[40] N. Zhao, and Z. Li, “Experiment and artificial neural network prediction of thermal conductivity and

viscosity for alumina-water nanofluids," *Materials*, vol. 10, no. 5, pp. 552, May 2017. DOI: 10.3390/ma10050552.

[41] C. K. Tan, J. Ward, S. J. Wilcox, and R. Payne, "Artificial neural network modelling of the thermal performance of a compact heat exchanger," *Appl. Therm. Eng.*, vol. 29, no. 17-18, pp. 3609–3617, Dec. 2009. DOI: 10.1016/j.applthermaleng.2009.06.017.

[42] M. Mohanraj, S. Jayaraj, and C. Muraleedharan, "Applications of artificial neural networks for thermal analysis of heat exchangers – A review," *Int. J. Therm. Sci.*, vol. 90, pp. 150–172, Apr. 2015. DOI: 10.1016/j.ijthermalsci.2014.11.030.

[43] M. Mohanraj, S. Jayaraj, and C. Muraleedharan, "Applications of artificial neural networks for refrigeration, air-conditioning and heat pump systems — A review," *Renew. Sust. Energy Reviews*, vol. 16, no. 2, pp. 1340–1358, Feb. 2012.

[44] K.-T. Yang, "Artificial neural networks (ANNs): A new paradigm for thermal science and engineering," *J. Heat Transf.*, vol. 130, no. 9, pp. 1–19, Sep. 2008. DOI: 10.1115/1.2944238.

[45] J. Krzywanski, and W. Nowak, "Modeling of heat transfer coefficient in the furnace of CFB boilers by artificial neural network approach," *Int. J. Heat Mass Transf.*, vol. 55, no. 15-16, pp. 4246–4253, Jul. 2012. DOI: 10.1016/j.ijheatmasstransfer.2012.03.066.

[46] D. R. E. Ewim, and J. P. Meyer, "Experimental investigation of condensation heat transfer coefficients in an inclined smooth tube at low mass fluxes," presented at the 16th International Heat Transfer Conference, IHTC-16, Beijing, China, Aug. 10–15, 2018. DOI: 10.1615/IHTC16.mpf.023113.

[47] S. N. R. Abadi, M. Mehrabi, and J. P. Meyer, "Prediction and optimization of condensation heat transfer coefficients and pressure drops of R134a inside an inclined smooth tube," *Int. J. Heat Mass Transf.*, vol. 124, pp. 953–966, Sep. 2018.

[48] A. O. Adelaja, J. Dirker, and J. P. Meyer, "Convective condensation heat transfer of R134a in tubes at different inclination angles," *Int. J. Green Energy*, vol. 13, no. 8, pp. 812–821, Mar. 2016. DOI: 10.1080/15435075.2016.1161633.

[49] A. O. Adelaja, J. Dirker, and J. P. Meyer, "Experimental study of the pressure drop during condensation in an inclined smooth tube at different saturation temperatures," *Int. J. Heat Mass Transf.*, vol. 105, pp. 237–251, Feb. 2017.

[50] M. Balcilar, A. Dalkilic, and S. Wongwises, "Artificial neural network techniques for the determination of condensation heat transfer characteristics during downward annular flow of r134a inside a vertical smooth tube," *Int. Commun. Heat Mass Transf.*, vol. 38, no. 1, pp. 75–84, Jan. 2011. DOI: 10.1016/j.icheatmasstransfer.2010.10.009.

[51] D. R. E. Ewim, and J. P. Meyer, "Pressure drop during condensation at low mass fluxes in smooth horizontal and inclined tubes," *Int. J. Heat Mass Transf.*, vol. 133, pp. 686–701, Apr. 2019. DOI: 10.1016/j.ijheatmasstransfer.2018.12.161.

[52] S. Lips, and J. P. Meyer, "Effect of gravity forces on heat transfer and pressure drop during condensation of R134a," *Microgravity Sci. Technol.*, vol. 24, no. 3, pp. 157–164, Jun. 2012. DOI: 10.1007/s12217-011-9292-3.

[53] A. O. Adelaja, D. R. E. Ewim, J. Dirker, and, and J. P. Meyer, "Experimental investigation on pressure drop and friction factor in tubes at different inclination angles during the condensation of R134a," presented at the 15th International Heat Transfer Conference, IHTC-15, Kyoto, Japan, Aug. 1-15, 2014. DOI: 10.1615/IHTC15.cds.009363.

[54] S. Lips, and J. P. Meyer, "Experimental study of convective condensation in an inclined smooth tube. Part II: Inclination effect on pressure drops and void fractions," *Int. J. Heat Mass Transf.*, vol. 55, no. 1-3, pp. 405–412, Jan. 2012.

[55] S. P. Olivier, J. P. Meyer, M. De Paepe, and K. De Kerpel, "The influence of inclination angle on void fraction and heat transfer during condensation inside a smooth tube," *Int. J. Multiph. Flow*, vol. 80, pp. 1–14, Apr. 2016. DOI: 10.1016/j.ijmultiphaseflow.2015.10.015.

[56] S. Lips, and J. P. Meyer, "Stratified flow model for convective condensation in an inclined tube," *Int. J. Heat Fluid Flow*, vol. 36, pp. 83–91, Aug. 2012.

[57] E. W. Lemmon, M. L. Huber, and, and M. O. McLinden, National Institute of Standards and Technology (NIST) reference database 23: Reference fluid thermodynamic and transport properties (REFPROP), version 9.1, Gaithersburg, MD, USA: REFPROP, May 7, 2013.

[58] R. Lipmann, "An introduction to computing with neural nets," *IEEE ASSP mag.*, vol. 4, no. 2, pp. 4–22, Apr. 1987. DOI: 10.1109/MASSP.1987.1165576.

[59] R. Tong, "A control engineering review of fuzzy systems," *Automatica*, vol. 13, no. 6, pp. 559–569, Nov. 1977. DOI: 10.1016/0005-1098(77)90077-2.

[60] S. Pesteei, and M. Mehrabi, "Modeling of convection heat transfer of supercritical carbon dioxide in a vertical tube at low reynolds numbers using artificial neural network," *Int," Commun. Heat Mass Transf.*, vol. 37, no. 7, pp. 901–906, Aug. 2010.

[61] J.-S. Jang, "ANFIS: adaptive-network-based fuzzy inference system," *IEEE Trans. Syst., Man, Cybern. Syst.*, vol. 23, no. 3, pp. 665–685, May/Jun. 1993. DOI: 10.1109/21.256541.

[62] D. Hanbay, A. Baylar, and E. Ozpolat, "Predicting flow conditions over stepped chutes based on ANFIS," *Soft Comput.*, vol. 13, no. 7, pp. 701–707, May. 2009.

[63] M. Mehrabi, S. M. Pesteei, and T. Pashaee G, "Modeling of heat transfer and fluid flow characteristics of helicoidal double-pipe heat exchangers using adaptive neuro-fuzzy inference system (ANFIS)," *Int," Commun. Heat Mass Transf.*, vol. 38, no. 4, pp. 525–532, Apr. 2011.

[64] M. Mehrabi, M. Sharifpur, and J. P. Meyer, "Application of the FCM-based neuro-fuzzy inference system and genetic algorithm-polynomial neural network approaches to modelling the thermal conductivity of alumina-water nanofluids," *Int. Commun. Heat Mass Transf.*, vol. 39, no. 7, pp. 971–977, Aug. 2012.

[65] M. Mehrabi, S. Rezazadeh, M. Sharifpur, and, and J. P. Meyer, "Modeling of proton exchange membrane fuel cell (PEMFC) performance by using genetic algorithm-polynomial neural network (GA-PNN) hybrid system, presented at ASME 2012 10th International Conference on Fuel Cell Science, Engineering and Technology (FUELCELL 2012), San Diego, CA, USA, Jul. 23-26, 2012. DOI: 10.1115/fuelcell2012-91391.

[66] M. Mehrabi, M. Sharifpur, and, and J. P. Meyer, "Adaptive neuro-fuzzy modeling of the thermal conductivity of alumina-water nanofluids," presented at ASME 2012 Third International Conference on Micro/Nanoscale Heat and Mass Transfer (MNHMT2012), Atlanta, GA, USA, Mar. 3-6, 2012. DOI: 10.1115/mnhmt2012-75023.

[67] M. Mehrabi, "Application of FCM-ANFIS approach to model heat transfer and pressure drop of titania-water nanofluids in the turbulent flow regime," presented at the 19th International Conference on Thermal, Mechanical and Multi-Physics Simulation and Experiments in Microelectronics and Microsystems (EuroSimE 2018), Toulouse, France, Apr. 15-18, 2018. DOI: 10.1109/EuroSimE.2018.8369927.

[68] M. Mehrabi, M. Sharifpur, and J. P. Meyer, "Modelling and multi-objective optimization of the convective heat transfer characteristics and pressure drop of low concentration tio2-water nanofluids in the turbulent flow regime," *Int. J. Heat Mass Transf.*, vol. 67, pp. 646–653, Dec. 2013. DOI: 10.1016/j.ijheatmasstransfer.2013.08.013.

[69] S. L. Chiu, "Fuzzy model identification based on cluster estimation," *J. Intell. Fuzzy Syst.*, vol. 2, no. 3, pp. 267–278, Jun 1994. DOI: 10.3233/IFS-1994-2306.

[70] M. Mehrabi, S. M. A. N. R. Abadi, and J. P. Meyer, "Heat transfer and fluid flow optimization of titanium dioxide-water nanofluids in a turbulent flow regime," *Heat Transf. Eng.*, vol. 41, pp. 36–49Nov. 2018. DOI: 10.1080/01457632.2018.1513623.

[71] J. C. Dunn, "A fuzzy relative of the ISODATA process and its use in detecting compact well-separated clusters," *J. Cybern*, vol. 3, no. 3, pp. 32–57, Apr. 1973.

[72] J. C. Bezdek, *Pattern Recognition with Fuzzy Objective Function Algorithms*. New York, NY, USA: Springer, 1981. DOI: 10.1007/978-1-4757-0450-1.

[73] J. C. Bezdek, R. Ehrlich, and W. Full, "FCM: The fuzzy C-means clustering algorithm," *Comput. Geosci.*, vol. 10, no. 2-3, pp. 191–203, Jan. 1984. DOI: 10.1016/0098-3004(84)90020-7.

Appendix

$$[\mathbf{a}_{i,j}] = \begin{bmatrix} 22.72 & -1092 & -66.57 & -16.74 & 2104 \\ 6.439 & 94.35 & -22.21 & 3.594 & 1618 \\ -85.32 & 1110 & 91.58 & -4.936 & 8869 \\ 5.991 & 2840 & -7443 & 15.69 & 6172 \\ -471.7 & -1.203 & 2214 & 3280 & -4.812 \\ -3.78 & -2337 & -26 & 12.06 & 3476 \\ 2.955 & 1059 & -0.3575 & 0.6704 & 693.9 \\ 2.975 & -184.3 & -4.198 & 5.384 & 1756 \\ 0.8524 & 88.59 & 9.916 & 3.157 & 1017 \\ 85.56 & 331.4 & -6.514 & 0.0001604 & -2996 \\ -9.019 & 1522 & -39.46 & 2.139 & 2029 \\ -3 & -558 & -73.18 & 5.393 & 2567 \\ 5.284 & 761.4 & 19.41 & 4.453 & 417.6 \\ 193.5 & 52.1 & -0.4729 & 4.179 & -17320 \\ -28.54 & 117.6 & 36.37 & 4.665 & 3900 \\ 7.364 & -1480 & -10.31 & 19.12 & 2530 \\ 1.325 & 411.2 & -6.14 & 21.85 & 2817 \\ 4.345 & 741.7 & -12.89 & 0.9427 & 912.7 \\ 0.645 & -1.957 & -1.728 & 23.06 & 3128 \\ 180.9 & 140.9 & 0.7634 & 21.17 & -10670 \\ 25.01 & 2955 & -34.13 & -6.349 & -2643 \\ -252.6 & -2476 & 3258 & 393.6 & -9906 \\ -107.8 & 1427 & -53.35 & -3.738 & 11940 \\ -113.4 & 428.6 & -15.51 & 20.74 & 8409 \\ 346.1 & -7288 & -343 & 46.21 & -19780 \\ -3.794 & 322.2 & -2.171 & -1.075 & 1906 \\ 0.3387 & 1174 & -23.68 & -0.1724 & 1245 \\ 191.8 & 2595 & -3.236 & 0.8429 & -14540 \\ -463.1 & -3.474 & 242.4 & -32.68 & -4.632 \end{bmatrix}$$